International Journal of Biochemistry and Cell Biology 113 (2019) 87–94

Contents lists available at ScienceDirect

International Journal of Biochemistry and Cell Biology

journal homepage: www.elsevier.com/locate/biocel

bFGF overexpression adipose derived mesenchymal stem cells improved the survival of pulmonary arterial endothelial cells via PI3k/Akt signaling pathway

Pengbo Wang[a,b], Jun Li[a], Caixin Zhang[a,b], Lin Luo[b], Songshi Ni[a,*], Zhiyuan Tang[a,*]

[a] Department of Respiratory and Critical Care Medicine, Affiliated Hospital of Nantong University, Nantong, 226001, Jiangsu, China
[b] Medical School of Nantong University, Nantong, Jiangsu, China

ARTICLE INFO

Keywords:
bFGF
ASC
HPAEC
PI3k/Akt
PAH

ABSTRACT

Pulmonary arterial hypertension (PAH) is characterized as pulmonary arterial endothelial dysfunction and endothelial cells over proliferation, therefore, the repair of pulmonary arterial endothelial cells has been a common goal in treating PAH. In the present study, human adipose derived mesenchymal stem cells (ASCs) were transfected with bFGF lentiviral vector and co-cultured with monocrotaline pyrrole treated human pulmonary arterial endothelial cells (HPAECs). The results showed that bFGF-ASCs improved the proliferation, viability and decreased the apoptosis of HPAECs, besides, improved PAH was observed in PAH rat models. Western blot analysis showed that the PI3k and p-Akt protein expression level increased in HPAECs, suggesting the activation of the PI3k/Akt signaling pathway. With the administration of LY294002, the bFGF induced HPAECs survival and PI3k/Akt signaling activation were successfully blocked. The present study demonstrated that bFGF transfected ASCs improved the survival of HPAECs by activating the PI3k/Akt pathway.

1. Introduction

Pulmonary arterial hypertension (PAH) is a rare, severe, and progressive disease with an estimated prevalence of ≈15 cases per million (Thenappan et al., 2012). The pathogenesis of PAH includes sustained vasoconstriction and abnormal progressive fixed vascular remodeling, this is accompanied by endothelial dysfunction and activation of fibroblasts and smooth muscle cells (Tuder et al., 2009). It is now accepted that injury to the endothelial cells of the pulmonary arteries is central for the subsequent development of lumen-obliterative lung vascular lesions. Therefore, the repair of pulmonary arterial endothelial cells has been a common goal in treating PAH.

Cell-based gene therapies have garnered increasing interest due to their beneficial roles in ameliorating the progression of PAH (Kanki-Horimoto et al., 2006; Luan et al., 2012). Human adipose tissue is an abundant and accessible source of adipose derived multipotent mesenchymal stem cells (ASCs), which hold great potential for therapeutic applications in regenerative medicine and tissue engineering (Karpov et al., 2017; Zuk et al., 2001). ASCs have been shown to be capable of reducing inflammation in damaged tissues, stimulating angiogenesis and reducing apoptosis (Chang et al., 2012; Gebler et al., 2012; Shin et al., 2013; Yanez et al., 2006).

Basic fibroblast growth factor (bFGF) is a representative growth factor which has shown the potential effects on the repair and regeneration of tissues (Hankemeier et al., 2005; Moya et al., 2010), previous report showed that bFGF induced cell proliferation after flia-specific gene transfer in mice (Dignass et al., 1994; Guan et al., 2018; Holland and Varmus, 1998; Jia et al., 2018; Murphy et al., 1990), while the role of bFGF in pulmonary arterial endothelial cells repair was poorly investigated. In this study, we transfected ASCs with bFGF lentiviral vector, and the role of bFGF overexpression ASCs in repairing human pulmonary arterial endothelial cells (HPAECs) was observed, and the aim of this study was to investigate the mechanism of bFGF in repairing the HPAECs, and to provide the theoretical foundation for PAH endothelial regeneration.

2. Materials and methods

2.1. Preparation of monocrotaline pyrrole (MCTP)

For use in cell culture, MCTP was prepared from monocrotaline (MCT) (Sigma, USA) by the method of Mattocks et al (Mattocks et al.,

* Corresponding authors at: Department of Respiratory and Critical Care Medicine, Affiliated Hospital of Nantong University, Xisi road 20th, Nantong City, 226001, Jiangsu Province, China.
E-mail addresses: jsntnss@163.com (S. Ni), tina2951@sina.com (Z. Tang).

https://doi.org/10.1016/j.biocel.2019.06.004
Received 28 February 2019; Received in revised form 6 June 2019; Accepted 10 June 2019
Available online 11 June 2019
1357-2725/

1989). With the use of mass analysis, 30–50% of the input MCT was converted to the pyrrolic derivative (data not shown). MCTP was stored in small aliquots in dimethylformamide (DMF) at −80 °C. Dose of MCTP applied in the experiment was conferred to a final concentration of 0.085 μg/ml (medium), MCTP was added directly to the culture medium with a rapid swirling motion, and the medium was changed 1 min later. Control cultures received an equivalent volume of DMF.

2.2. Cells and co-culture

The human ASCs were a kind gift from the Genesis stem cell regeneration medicine Co, Ltd. (Jiangsu, China). Breast adipose lipoaspirates of human donors was used for ASCs isolation after informed consent was obtained by Genesis. Briefly, 60 to 120 ml of the raw lipoaspirates was washed with phosphate-buffered saline (PBS) and enzymatically digested with 0.1% collagenase type I (Sigma, USA) at 37 °C for 1 h. The digested lipoaspirates were centrifuged at 400 g for 15 min, and the pellet was resuspended and passed through a 100 μm mesh filter to remove debris. Subsequently, 1 × 10^6 cells were plated in T-75 culture flasks in ASC medium (Haoyang, China) and incubated at 37 °C in a humidified 5% CO2 atmosphere. The medium was changed twice weekly, and cells were passaged with 0.25% trypsin/0.1% EDTA upon reaching 90% confluency. Experiments were performed at passages 3–4. The employment of human ASCs was approved by the ethic committee of affiliated hospital of Nantong University (review number 2018-L129). Human pulmonary arterial endothelial cells (HPAECs) were purchased from Bena Culture Collection (Nanjing, China). Cells were cultured in T-75 flasks, and HPAECs in Dulbecco's modified Eagle's medium (DMEM) containing 10% FBS (Sabrina, South America), 1% penicillin/streptomycin (Sigma USA); ASCs were cultured in TheraPEAK Chemically Defined Mesenchymal Stem Cell Growth Medium containing supplements and growth factors (Lonza) at 37 °C in a humidified 5% CO2 atmosphere, and were grown to 80–90% confluence. Cells were then divided into HPAECs control group (Con), MCTP-HPAECs group (MCTP), ASCs + MCTP-HPAECs co-culture group (ASC), bFGF-ASCs + MCTP-HPAECs co-culture group (bFGF) and bFGF-NC-ASCs + MCTP-HPAECs co-culture group (NC). 1 × 10^4 HPAECs and 1 × 10^4 ASCs were incubated in six-well plates and transwells respectively, DMEM was used for co-culture. MCTP or DMF (for control HPAECs treatment) was added to treat HPAECs directly. Transwells were then set into the HPAECs wells after the treatment and were co-cultured for 72 h at an atmosphere of 5% CO2, 37 °C.

2.3. bFGF lentiviral vector construction and ASC transfection

Human bFGF-GFP-lentiviral (Gene Bank accession NM_002006) and the negative control (NC) were constructed by the Vigene bioscience (Shandong, China). ASC cultures were gently dissociated with 0.05% Trypsin-EDTA to single cell suspension, washed, counted, and plated for 24 h in a 24-well plate (25,000 cells/50 μl). ASCs were transfected with bFGF-GFP-lentiviral at a multiplicity of infection of 50. The medium was changed 12 h after the transfection, and transduction efficiency and expression of bFGF were examined 48 h after transfection by fluorescence microscopic visualization of GFP (Leica, Wetzlar, Germany). Transfected ASCs were then passaged and collected for co-culture.

2.4. Crystal violet staining

For HPAECs proliferation analysis, HPAECs of all groups were fixed with 10% paraformaldehyde and stained with 0.5% crystal violet (Sigma-Aldrich, St. Louis, MO, USA) for 20 min. Cells were washed with distilled water and the plates were scanned after drying.

2.5. Cell viability assay

HPAECs viability was assessed using a CCK-8 Kit (Beyotime, China). In summary, cells were grouped as aforementioned, incubated for 72 h, then, the medium was replaced by 400 μl fresh medium and 40 μl of CCK-8 in each well. The HPAECs were incubated for another 3 h. Cell viability was determined by measuring the absorbance at 450 nm using a microplate reader (BioTek, USA). Assays included six replicates per experimental groups.

2.6. HPAECs apoptosis analysis using flow cytometry

To evaluate the apoptosis of HPAECs in different co-culture groups, Annexin V-PI apoptosis detection kit (Beyotime biotechnology, China) was used by following the manufacturer's protocol. Cells were grouped into ASCs + MCTP-HPAECs co-culture group (ASC), bFGF-ASCs + MCTP-HPAECs co-culture group (bFGF) and bFGF-NC-ASCs + MCTP-HPAECs co-culture group (NC), incubated for 72 h. HPAECs were harvested and centrifuged at 1000 g for 5 min, then the pellet was resuspended in 195 μl of the sample solution and transferred to a 5 ml FACS tube, incubated with 5 μl of annexin V and 10 μl of PI for 15 min at room temperature in the dark, then, the samples were analyzed by flow cytometry (Becton Dickinson) using Cell Quest Research Software (Becton Dickinson). Assays included three replicates per experimental groups.

2.7. Western blotting

The relative expression of bFGF, PI3k, Akt and p-Akt were studied using western blotting. HPAECs were collected 72 h after the co-culture, HPAECs protein samples were separated in SDS-PAGE gels using a standard protocol. An Anti-human bFGF antibody(1 : 1000, Sigma), anti-PI3k (p85) antibody (1 : 1000, Cell Signaling Technology), anti-Akt antibody (1 : 1000, Cell Signaling Technology), anti-pAkt (Ser473) antidody (1 : 1000, Cell Signaling Technology), anti-GAPDH antibody (1 : 1000, Beyotime biotechnology, China) and antiβ-actin antibody (1 : 1000, Beyotime biotechnology, China) were used as primary antibodies. The membranes were incubated for 2 h with an anti-rabbit HRP-linked secondary antibody (1 : 2000, abcam). The relative protein levels were calculated by quantification of band intensity with an Odyssey infrared imaging system (Li-Co Biosciences) and normalized to GAPDH or β-actin.

2.8. PI3k/Akt pathway inhibition

To assess the role of PI3k/Akt pathway in bFGF-ASCs induced HPAECs proliferation, HPAECs were pretreated with 25 μM of LY294002 (Beyotime, China) in complete medium for 12 h, then, HPAECs were assigned to the MCTP-HPAECs (LY294002 +) + bFGF-ASCs co-culture group and the MCTP-HPAECs (LY294002-) + bFGF-ASCs co-culture group. HPAECs of both co-culture groups were subjected to CCK-8 cell viability assay and western bloting analysis. Assays included three replicates per experimental groups.

2.9. Animals and experimental design

Twelve-week old male, Sprague-Dawley rats, weighing 180–200 g (SPF), provided by the experimental animal center of Nantong University, were given food and water ad libitum under constant conditions (12:12 h light: dark cycle, 60% humidity at 22 ± 2 °C). Animal experiments were performed in accordance with the ethical standards provided by the responsible committee of the institution at which the work was carried out and in accordance with the Declaration of Helsinki (as revised in Edinburgh 2000). This study was approved by the Committee on Animal Care of Nantong University. All animal experiments were performed by strictly following the IACUC procedures

Rats were randomly divided into three groups: the PAH model group (Con, n = 6), the ASCs transplanted group (ASC, n = 6) and the bFGF-ASCs transplanted group (bFGF, n = 6). Animals were

intraperitoneally injected with MCT (60 mg/kg). MCT was dissolved in 1 N HCl (the pH was adjusted to 7.4). Two weeks after the MCT injection, rats of the ASC and bFGF groups followed a right jugular vein injection of 3 × 10^6 ASCs or bFGF-ASCs respectively (cells were diluted in 200 μl PBS), the Con received an equal volume of PBS. Four weeks after the MCT injection, all rats were subjected to the following experiments.

2.10. RNA extraction and quantitative real-time PCR

To evaluate the mRNA expression in each cell group, rt-PCR was performed. Total RNA in HPAECs was isolated by using Trizol reagent (LifeTechnologies, USA) according to the manufacturer's instructions. cDNAs were then synthesized using Revertaid First Strand cDNA Synthesis KIT(Thermo scientific, USA). Up to 1 μL of cDNA was used as a template for the specific PCR reactions. The primers used were synthesized by Biomics Biotechnology (Jiangsu, China), as follows: 18 s forward5'-ACCACGCAGAGTACACGCG-3' and reverse 5'-CAACCCCTG GATGCATCTGGA-3', PI3K, forward 5'-GTAAGCAGGGCTGCTATGCC-3' and reverse 5'-CCTTGGGTGGCTTGAAGGTG-3'; Akt, forward 5'-TTCT GCAGCTATGCGAATGTG-3' and reverse 5'-TGGCCAGCATACCATAGT GAGGTT-3'. Each assay was performed in triplicate. PCR reactions were carried out using SYBR Green qPCR Master Mix (Thermo scientific, USA) according to the manufacturer's instructions. The results were analyzed with ABI 7500 RealTimePCR System software. The level of 18 s was used as an internal standard.

2.11. Measurement of right ventricular systolic pressure

All rats were anesthetized with 3% sodium pentobarbital (30 mg/kg, i.p.) at the end of the fourth week. Rats were kept in a supine position, a vertical incision was made on the right side of the neck, and 1.5 cm of the right jugular vein was isolated, anticoagulated with 1% heparin saline (1 mg/kg, i.p.), the distal end was ligated, a PE-50 polyethylene tube (0.58 mm × 0.99 mm) filled with heparin saline was inserted 1 cm deep, systolic and diastolic blood pressures were recorded by the BIOPAC multileads physiograph. The catheter was then further inserted into the right ventricle, systolic pressure was recorded. Each value was recorded every 1 min for a period of 10 s and altogether 50 s was recorded to calculate an average value.

2.12. Right ventricle hypertrophy determination

Hearts were collected, right ventricle (R) was dissected from left ventricle and septa (L + S). R and L + S weights were measured, and right ventricle hypertrophy was assessed by the ratio of R/L + S.

2.13. Histology and immunohistochemistry assay

Lung tissue from the right upper lobe was fixed with 4% paraformaldehyde, dehydrated and embedded in paraffin. The tissue was sectioned into 4 mm slices, and stained with hematoxylin-eosin for evaluation of endothelial proliferation. Pulmonary arterioles between 50 and 200 μm in external diameter were chosen for morphological analysis. Atleast 5 visions of each slice were captured with light microscope (Leica, Solms, Germany) and analyzed using the Image Pro Plus 6.0 software (Media Cybernetics, Inc.).

Immunohistochemistry (IHC) was performed on formalin-fixed paraffin-embedded tissue. The primary antibodies were the same as those used for western blot analysis. The Vector Laboratories ImmPRESS Detection kit was employed for visualizing the reacted antibody, which employed a second antibody conjugated with horseradish peroxidase and a diaminobenzidine -based stain. All sections were counterstained with Mayer's hematoxylin. For each rat, three separate slides were analyzed. Images were captured under a light microscope at 100× magnification. Image Pro Plus 6.0 software was used to analyze the staining intensity. Five microscopic fields in tissues were randomly selected and the integral optical density (IOD) of bFGF, PI3k, and p-Akt was calculated, and this was considered as the expression level. Higher IOD values represented higher antigen expression, and vice versa.

2.14. Statistical analyses

The results were analyzed with the statistical software of STATA 7.0 software (Stata, College Station, TX, USA). All data were presented as Mean ± standard deviation. For parametric data, comparisons between groups were examined statistically using homogeneity of variance test and one-way ANOVA. $P < 0.05$ was considered significant.

3. Results

3.1. bFGF expression in ASCs

Human ASCs were infected with bFGF-GFP lentiviral as aforementioned. The bFGF expression in ASCs was evaluated by fluorescence microscopic visualization of GFP and western blotting 48 h after the transfection. The bFGF expression level in the bFGF transfected ASCs was significantly higher than those in the control ASCs and the NC-ASCs (Fig. 1). These results demonstrated that a recombinant lentiviral vector harboring the bFGF gene could successfully transfer into ASCs and efficiently increase the bFGF expression in ASCs.

3.2. bFGF-ASCs improved the proliferation of MCTP treated HPAECs

To evaluate the effect of bFGF-ASCs on HPAECs proliferation, HPAECs were subjected to crystal violet staining. Compared to the control group (HPAECs), treatment with MCTP resulted in a significant decrease in total cell counts (204.4 ± 32.11 vs 126.3 ± 18.38). In contrast, co-culture of HPAECs with ASCs resulted in a significant increase in total cell counts compared to HPAECs individual control (288.9 ± 20.85 vs 204.4 ± 32.11), and the presence of ASCs also mitigated cell loss resulting from exposure to MCTP to a significant extent (288.9 ± 20.85 vs 126.3 ± 18.38); the bFGF-ASCs were observed to be even potent in increasing the cell counts, as comapred to HPAECs individual control (500.8 ± 31.19 vs 204.4 ± 32.11), and compared to MCTP treated HPAECs (500.8 ± 31.19 vs 126.3 ± 18.38) (Fig. 2a–f).

3.3. bFGF-ASCs improved the viability and decreased the apoptosis of HPAECs

To evaluate the effect of bFGF-ASCs on HPAECs viability and apoptosis, CCK-8 and flow cytometric analyses were performed. CCK-8 results showed that compared to the HPAECs control group (Con), treatment with MCTP resulted in a significant decrease in HPAECs viability ($p < 0.05$), ASCs ameliorated the decrease resulting from exposure to MCTP and increased the HPAECs viability ($p < 0.01$), bFGF-ASCs were even more potent in increasing the cell viability ($p < 0.01$) (Fig. 2g).

Results from the flow cytometry showed that compared to ASCs co-culture group, bFGF-ASCs significantly decreased both the early and late apoptosis of HPAECs (($p < 0.01$) (Fig. 3).

3.4. bFGF-ASCs improved PAH and right ventricular hypertrophy in rats

Compared to the model group (Con), ASCs treatment decreased the right ventricular systolic pressure (RVSP) and R/L + S ($p < 0.05$), bFGF-ASCs treatment even more significantly decreased RVSP and R/L + S ($p < 0.01$) (Fig. 4). Suggesting that ASCs treatment improved PAH, while the bFGF transfected ASCs played a even powerful role in improving PAH.

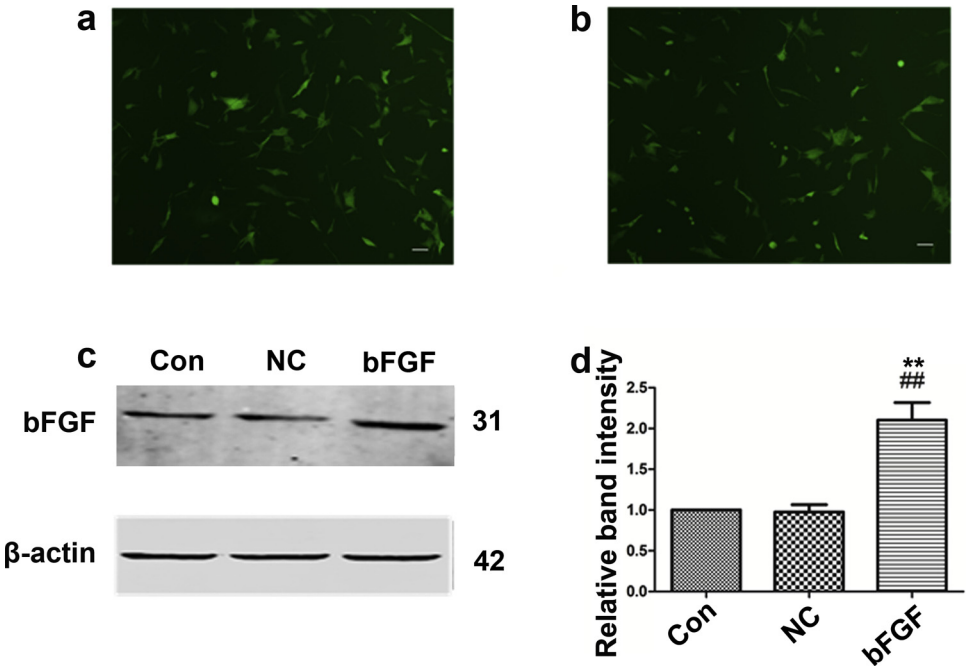

Fig. 1. bFGF lentiviral transfected ASCs improved in protein expression of bFGF.
(a): Representative image of bFGF lentiviral transfection. (b): Representative image of bFGF negative control lentiviral transfection. The original magnification is ×100. Scale bars, 50 μm. (c): Protein expression of bFGF. (d): Quantitative evaluation of band intensity. The protein expression level was normalized to GAPDH, the Con was set at 1, data represented the mean ± S.D. n = 3. vs. Con; **P < 0.01, vs. NC; ##P < 0.01. Con: ASCs control, NC: bFGF negative control transfected ASCs, bFGF: bFGF transfected ASCs.

3.5. bFGF-ASCs attenuated the MCT induced pulmonary arteriole endothelial proliferation by regulating the expression of PI3k and p-Akt

To assess the hyperproliferation of pulmonary artery, Hematoxylin-eosin staining was performed. Results showed that compared to the model group (Con), both ASCs transplanted groups decreased in the pulmonary arteriole endothelial thickness, the decrease was more obvious in bFGF-ASCs treated group than in the ASCs treated group ($p < 0.05$) (Fig. 5a, b). IHC rsults showed that compared to the model group, both ASCs transplanted group increased in the expression of bFGF, PI3k, and p-Akt; compared to the ASCs treated group, the expression level was even higher in the bFGF-ASCs treated group ($p < 0.05$) (Fig. 5a, c, d, e).

3.6. PI3k/Akt signaling pathway is essential for the role of bFGF

To determine whether bFGF-ASCs induced HPAECs proliferation was dependent on PI3k/Akt signaling pathway. Western-blot was performed. Compared to the HPAECs control group, the presence of bFGF-ASCs significantly increased the expression level of both PI3k and p-Akt ($p < 0.01$), the ASCs co-culture group ($p < 0.01$), and the NC-ASC co-culture group ($p < 0.01$) (Fig. 6). With the application of LY249002, a specific PI3k inhibitor, compared to the LY294002- group, the LY294002+ group significantly decreased in the expression of PI3k and p-Akt, the PI3k/Akt pathway was effectively blocked (Fig. 7a, b, c, d). Results of the HPAECs viability assay showed that compared to the HPAECs (LY294002-), HPAECs (LY294002+) decreased in cell viability ($p < 0.05$) (Fig. 7e). These results verified the pivotal role of PI3k/Akt pathway in bFGF mediated HPAECs survival and proliferation.

3.7. bFGF-ASCs did not regulate the mRNA expression of PI3k/Akt in HPAECs

To further clarify the mechanism of bFGF-ASCs inducing HPAECs proliferation, we thus performed rt-PCR by using the HPAECs samples from different co-culture groups. Results showed that no statistical difference was observed in PI3k/Akt mRNA expression among all HPAECs samples, suggesting that bFGF-ASCs did not improve HPAECs proliferation by regulating PI3k/Akt signaling pathway at the transcription level.(Fig. 8)

4. Discussion

PAH is characterized by over proliferation of the pulmonary endothelial, which contribute to the plexiform lesions and vascular occlusion (Abe et al., 2010; Cool et al., 2005; Tuder et al., 2001). Endothelial dysfunction and proliferation are at the root of vascular remodeling in PAH (Lee et al., 1998; Masri et al., 2007; Rabinovitch, 2012, Tuder et al., 2001, Tuder et al., 1994). The mechanisms responsible for pulmonary vascular endothelial proliferation in PAH remain poorly understood. Mesenchymal stem cells (MSCs) are regarded as attractive candidates for clinical repair or regeneration of damaged

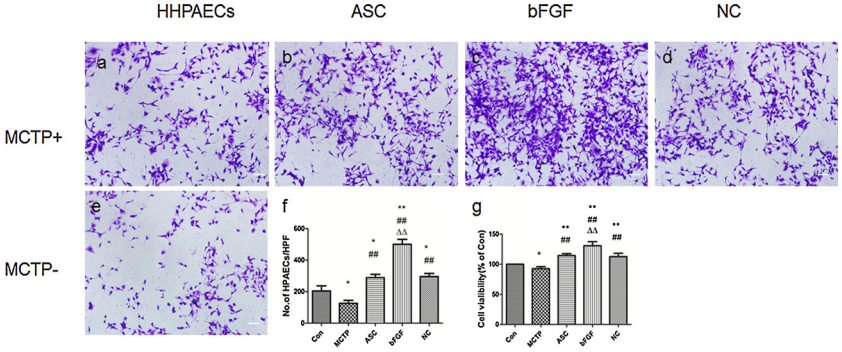

Fig. 2. bFGF-ASCs improved the proliferation and viability of MCTP treated HPAECs. (a–e): Representative images of HPAEC. The original magnification is ×100. Scale bars, 50 μm. (f): Number of cell count. Values represented mean ± S.D. At least ten visions from three replicates of each group were obtained. (g): Results of CCK-8. The Con was set at 100, data represented mean ± S.D. of six replicates. vs. Con; * P < 0.05, ** P < 0.01, vs. MCTP; ##P < 0.01, vs. ASC; ΔΔP < 0.01. Con: HPAECs control group, MCTP: MCTP-HPAECgroup, ASCs: ASCs + MCTP-HPAECs co-culture group, bFGF: bFGF-ASCs + MCTP-HPAECs co-culture group, NC: NC-ASCs + MCTP-HPAECs co-culture group.

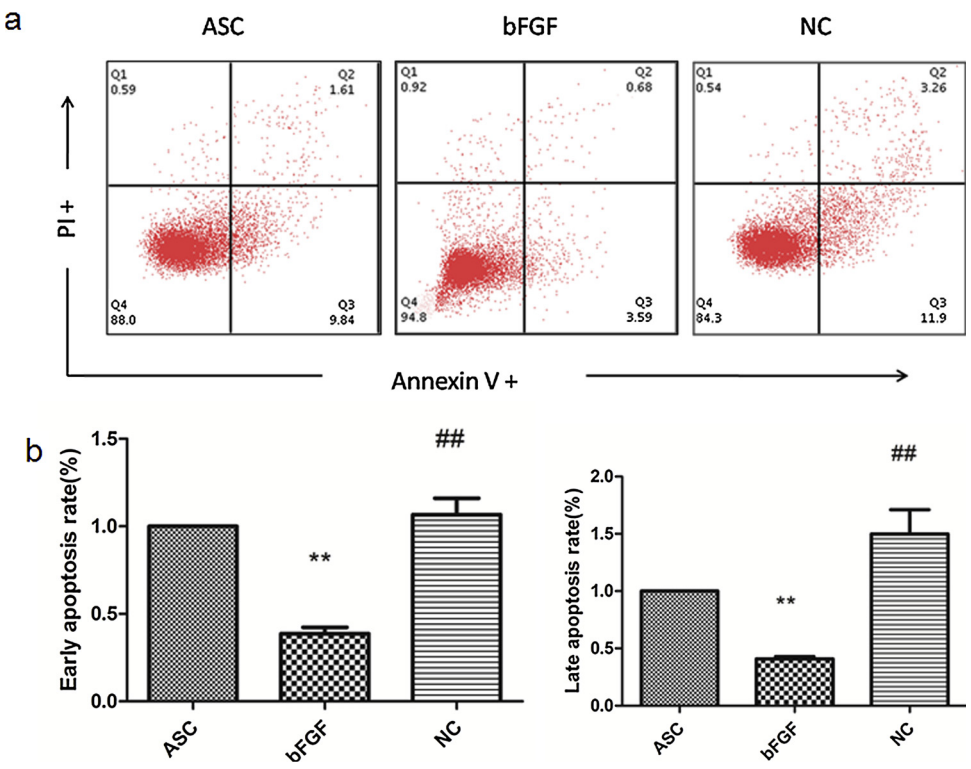

Fig. 3. bFGF overexpression ASCs decreased the apoptosis of HPAECs.
(a) Typical patches of apoptotic cells double stained with PI and Annexin V were acquired from three flow cytometric analyses. (b) Apoptotic cells indicated by early apoptosis (Annexin V + /PI–, Q3) and late apoptosis (Annexin V + /PI + , Q2). The ASC was set at 1, results were presented as mean ± S.D. and depict three independent experiments. vs. ASC; ** $p < 0.01$, vs. bFGF; ## $p < 0.01$. ASC: HPAECs + MCTP-ASCs co-culture group, bFGF: MCTP-HPAECs + bFGF-ASCs co-culture group, NC: MCTP-HPAECs + NC-ASCs co-culture group.

tissues, meanwhile, bFGF maintains the stemness of MSCs from a variety of species by prolonging their viability in culture (Tsutsumi et al., 2001). bFGF was reported to be capable of inducing cell proliferation in endothelial cell (Guan et al., 2018), epithelial cell (Dignass et al., 1994), fibroblast cell (Jia et al., 2018) and neural stem cell (Murphy et al., 1990). Previous studies administered the bFGF directly in their study, like other growth factors. However, free-bFGF was readily degradable in vivo, leading to loss of biological activity and functions (Andreopoulos and Persaud, 2006; Cai et al., 2005; Freudenberg et al., 2009). To gain satisfactory performance, bFGF was generally adsorbed onto or encapsulated within materials to secure biological activity in a sustained and controllable manner. We hypothesized that the combination of gene and cell therapies would accelerate HPAECs repair, and may be more effective than individual growth factors given systemically.

In the present study we constructed the bFGF lentiviral vector, and achived the bFGF overexpression ASCs by transfection. The results presented that bFGF transfected ASCs can effectively increase the HPAECs survival, proliferation and decrease the apoptosis. The PI3k/Akt pathway is a survival pathway that regulates cell proliferation, apoptosis, differentiation and migration (Zhang et al., 2013). Furthermore, PI3k/Akt pathway was the well documented downstream signaling of bFGF (Shi et al., 2015; Virag et al., 2007; Wang et al., 2015). The PI3k/Akt pathway was reported to play key roles in the physiology and pathophysiology of several types of cells (Liu et al., 2009; Martelli et al., 2010; Weichhart and Saemann, 2008; Zhao et al., 2012). PI3k functions by converting phosphatidylinositol 4,5-biphosphate to phosphatidylinositol 3,4,5-triphosphate, which binds both Akt and 3-phosphoinositide-dependent protein kinase 1 (PDK1), enabling PDK1 to phosphorylate Akt (Cantley, 2002; Liu et al., 2009). Akt as the primary downstream target protein of PI3k is then activated. The activation of Akt causes a cascade of responses with downstream targets that regulate cellular functions. Therefore, we sought to determine whether bFGF-ASCs induced cell survival and proliferation were dependent on PI3k/Akt pathway. Our results showed that the expression levels of PI3K mRNA, Akt mRNA in HPAECs did not change in the ASC and bFGF-ASC groups as compared to the control group, while bFGF significantly stimulated PI3k/Akt pathway as expressed by enhanced protein levels of PI3k and p-Akt in HPAECs and PAH rat models. Significant decrease in HPAECs viability was observed as the PI3k/Akt pathway was blocked by LY294002, suggesting that the pivotal role of PI3k/Akt pathway in bFGF mediated cell proliferation.

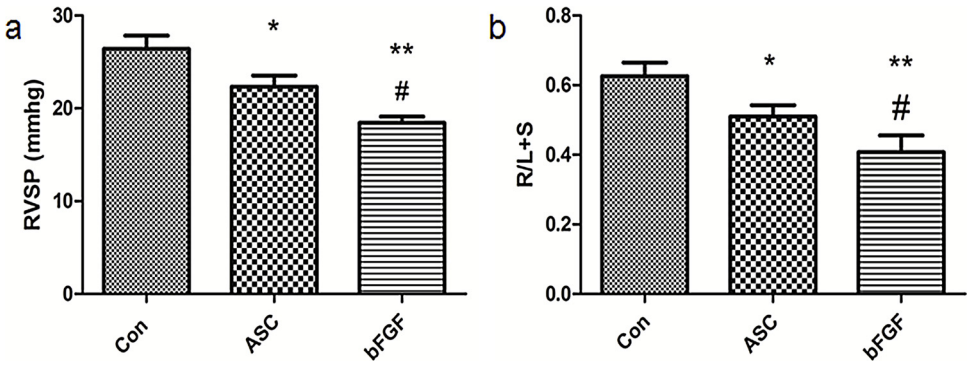

Fig. 4. bFGF-ASCs improved the MCT induced PAH and right ventricular hypertrophy in rats.
(a) Right ventricular systolic blood pressure (RVSP). (b) The R/L + S weight ratio. Data represented mean ± S.D. vs. Con; * $p < 0.05$, ** $p < 0.01$, vs. ASC; # $p < 0.05$. Con: PAH model group (n = 6), ASC: ASCs transplanted group (n = 6), bFGF: bFGF-ASCs transplanted group (n = 6).

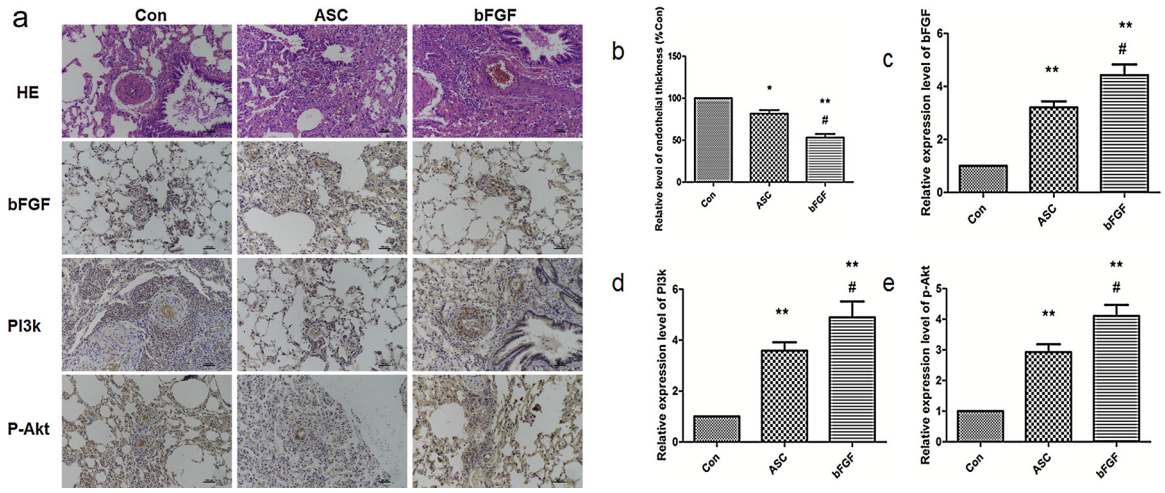

Fig. 5. bFGF-ASCs attenuated the MCT induced pulmonary arteriole hypertrophy.
(a) Representative images of Hematoxylin-eosin staining and IHC. The original magnification was × 200, Scale bars, 50 μm. (b) Relative level of arteriole endothelial thickness. (c) Relative level of bFGF. The control was set at 100, the values denote the relative length ± S.D. (d) Relative level of PI3k. (e) Relative level of p-Akt. Data represented mean ± S.D. The control was set at 1. vs. Con; * $p < 0.05$, ** $p < 0.01$, vs. ASC; # $p < 0.05$. Con: PAH model group (n = 6), ASC: ASCs transplanted group (n = 6), bFGF: bFGF-ASCs transplanted group (n = 6).

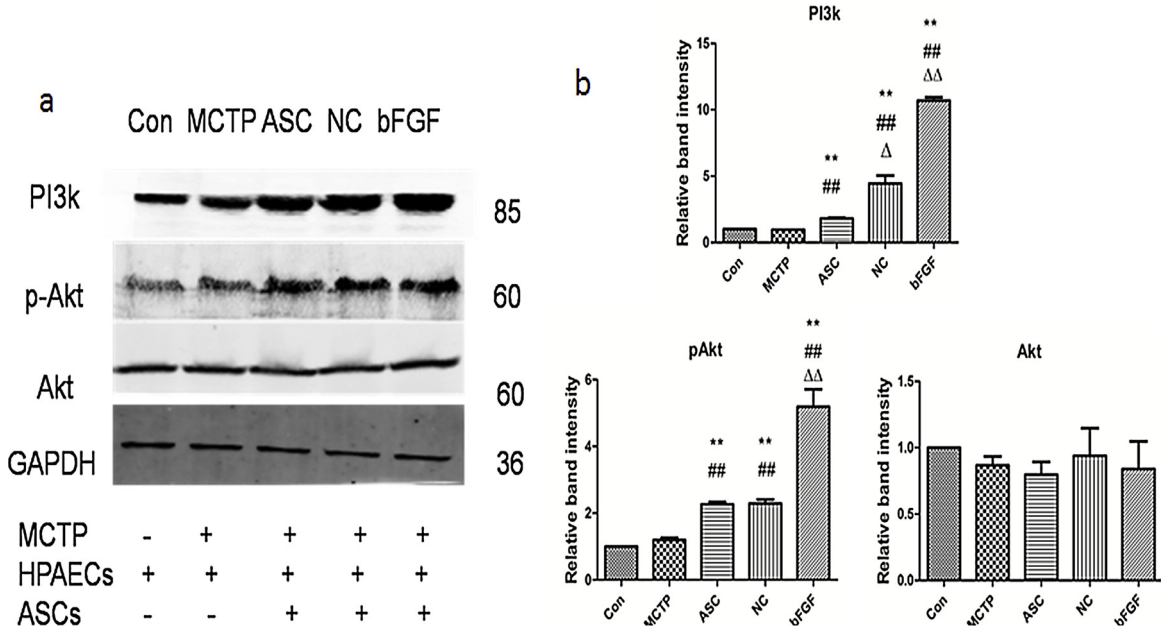

Fig. 6. bFGF-ASCs significantly increased the protein level of PI3k and p-Akt in HPAECs. (a): Protein expression. (b): Quantitative evaluation of band intensity. The band intensity was normalized to GAPDH, data represented mean ± S.D., n = 3. vs. Con; ** $p < 0.01$, vs. MCTP; ## $p < 0.01$,vs. ASC; Δ $P < 0.05$, ΔΔ $P < 0.01$. Con: HPAECs control, MCTP: MCTP treated HPAECs, ASCs: ASCs + MCTP-HPAECs co-culture group, NC: bFGF negative control co-culture group, bFGF: bFGF-ASCs + MCTP-HPAECs co-culture group.

5. Conclusion

In summary, our study showed that bFGF lentiviral transfected ASCs functioned in pulmonary endothelial repair via regulation of the PI3k/Akt signaling pathway, which provided a new perspective in PAH endothelial regeneration.

Limitations

The limitations of the present study must be taken into consideration. both MCTP treated HPAECs and MCT induced PAH rat models can not mimic the entire complex endothelial features observed in human PAH.

Statement of ethics

The employment of human ASCs was approved by the ethic committee of affiliated hospital of Nantong University (review number 2018-L129).

Disclosure statement

The authors have no conflicts of interest to declare.

Funding sources

This work was supported by the following grants: Youth Subject of Jiangsu Provincial Commission of Health and Family Planning [grant

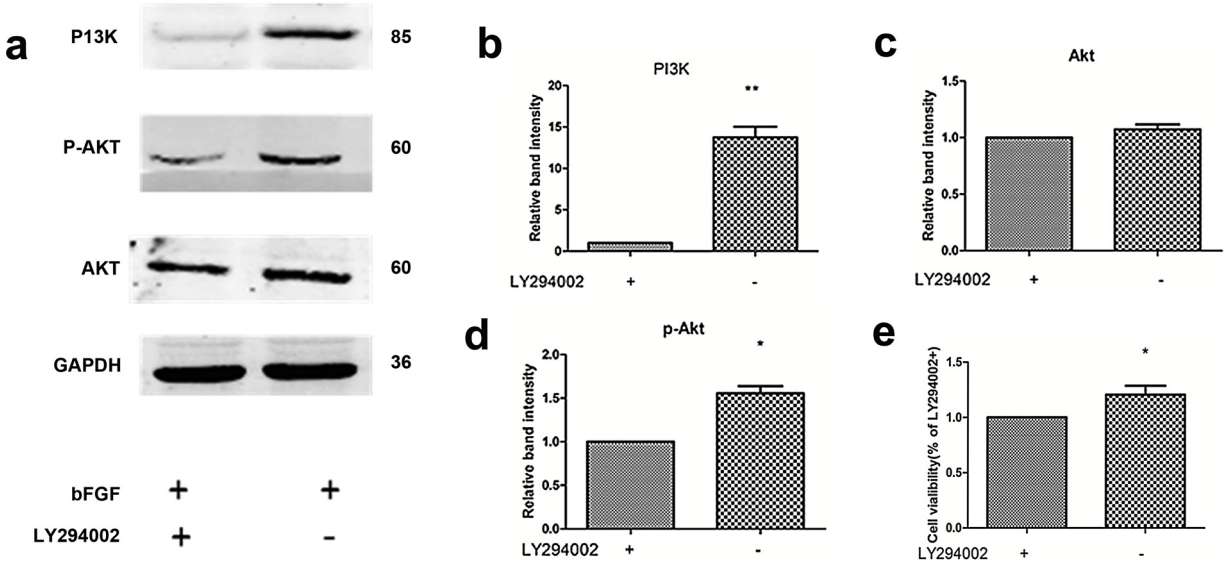

Fig. 7. LY294002 blocked the bFGF activated PI3k/Akt pathway and decreased the cell viability. (a): Protein expression. (b): Quantitative evaluation of band intensity of PI3k. (c): Quantitative evaluation of band intensity of Akt. (d): Quantitative evaluation of band intensity of p-Akt. (e): Results of CCK-8. LY294002+ was set at 1, data represented mean ± S.D., n = 3. vs. LY294002+; * $p < 0.05$, ** $p < 0.01$. LY294002+: bFGF-ASC + MCTP-HPAEC co-culture group with LY294002, LY294002-: bFGF-ASC + MCTP-HPAEC without LY294002.

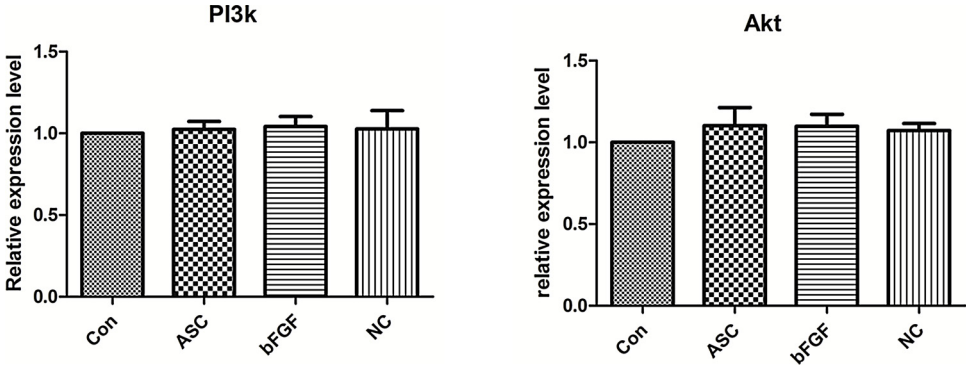

Fig. 8. bFGF-ASCs did not regulate the mRNA expression of PI3k/Akt in HPAECs.
Relative expression level of PI3k mRNA and Akt mRNA. Con was set at 1, the expression level was normalized to Con, data represented mean ± S.D., n = 3. Con: HPAECs control, ASCs: ASCs + MCTP-HPAECs co-culture group, bFGF: bFGF-ASCs + MCTP-HPAECs co-culture group, NC: bFGF negative control co-culture group.

number Q2017009]; Postgraduate Student Research and Practise Innovation Project of Jiangsu Province [grant number KYCX17-1935]; Key Technology Research of Nantong People's Livelihood [grant number MS32015025]; National Natural Science Foundation of China [grant number 81503143]; Six Talent Peaks Project in Jiangsu Province [No. 2015- WSW-049; 2015-WSN-062].

Acknowledgements

We are grateful for the Genesis stem cell regeneration medicine Co, Ltd (Jiangsu China) for their kindness of sharing the ASCs applied in the study. The Affiliated Hospital of Nantong University is the officially appointed co-operation hospital of Genesis in Jiangsu province, China, and was anthorized to carry on experiments on the stem cells isolated by Genesis.

Appendix A. Supplementary data

Supplementary material related to this article can be found, in the online version, at doi:https://doi.org/10.1016/j.biocel.2019.06.004.

References

Abe, K., Toba, M., Alzoubi, A., Ito, M., Fagan, K.A., Cool, C.D., et al., 2010. Formation of plexiform lesions in experimental severe pulmonary arterial hypertension. Circulation 121, 2747–2754.

Andreopoulos, F.M., Persaud, I., 2006. Delivery of basic fibroblast growth factor (bFGF) from photoresponsive hydrogel scaffolds. Biomaterials 27, 2468–2476.

Cai, S., Liu, Y., Zheng Shu, X., Prestwich, G.D., 2005. Injectable glycosaminoglycan hydrogels for controlled release of human basic fibroblast growth factor. Biomaterials 26, 6054–6067.

Cantley, L.C., 2002. The phosphoinositide 3-kinase pathway. Science 296, 1655–1657.

Chang, C.L., Leu, S., Sung, H.C., Zhen, Y.Y., Cho, C.L., Chen, A., et al., 2012. Impact of apoptotic adipose-derived mesenchymal stem cells on attenuating organ damage and reducing mortality in rat sepsis syndrome induced by cecal puncture and ligation. J. Transl. Med. 10, 244.

Cool, C.D., Groshong, S.D., Oakey, J., Voelkel, N.F., 2005. Pulmonary hypertension: cellular and molecular mechanisms. Chest 128 (565) S-71S.

Dignass, A.U., Tsunekawa, S., Podolsky, D.K., 1994. Fibroblast growth factors modulate intestinal epithelial cell growth and migration. Gastroenterology 106, 1254–1262.

Freudenberg, U., Hermann, A., Welzel, P.B., Stirl, K., Schwarz, S.C., Grimmer, M., et al., 2009. A star-PEG-heparin hydrogel platform to aid cell replacement therapies for neurodegenerative diseases. Biomaterials 30, 5049–5060.

Gebler, A., Zabel, O., Seliger, B., 2012. The immunomodulatory capacity of mesenchymal stem cells. Trends Mol. Med. 18, 128–134.

Guan, D., Mi, J., Chen, X., Wu, Y., Yao, Y., Wang, L., et al., 2018. Lung endothelial cell-targeted peptide-guided bFGF promotes the regeneration after radiation induced lung injury. Biomaterials 184, 10–19.

Hankemeier, S., Keus, M., Zeichen, J., Jagodzinski, M., Barkhausen, T., Bosch, U., et al., 2005. Modulation of proliferation and differentiation of human bone marrow stromal cells by fibroblast growth factor 2: potential implications for tissue engineering of tendons and ligaments. Tissue Eng. 11, 41–49.

Holland, E.C., Varmus, H.E., 1998. Basic fibroblast growth factor induces cell migration and proliferation after glia-specific gene transfer in mice. Proc. Natl. Acad. Sci. U. S. A. 95, 1218–1223.

Jia, Y.Y., Zhou, J.Y., Chang, Y., An, F., Li, X.W., Xu, X.Y., et al., 2018. Effect of optimized concentrations of basic fibroblast growth factor and epidermal growth factor on proliferation of fibroblasts and expression of collagen: related to pelvic floor tissue regeneration. Chin. Med. J. 131, 2089–2096.

Kanki-Horimoto, S., Horimoto, H., Mieno, S., Kishida, K., Watanabe, F., Furuya, E., et al., 2006. Implantation of mesenchymal stem cells overexpressing endothelial nitric oxide synthase improves right ventricular impairments caused by pulmonary hypertension. Circulation 114, I181–5.
Karpov, A.A., Udalova, D.V., Pliss, M.G., Galagudza, M.M., 2017. Can the outcomes of mesenchymal stem cell-based therapy for myocardial infarction be improved? Providing weapons and armour to cells. Cell Prolif. 50.
Lee, S.D., Shroyer, K.R., Markham, N.E., Cool, C.D., Voelkel, N.F., Tuder, R.M., 1998. Monoclonal endothelial cell proliferation is present in primary but not secondary pulmonary hypertension. J. Clin. Invest. 101, 927–934.
Liu, P., Cheng, H., Roberts, T.M., Zhao, J.J., 2009. Targeting the phosphoinositide 3-kinase pathway in cancer. Nat. Rev. Drug Discov. 8, 627–644.
Luan, Y., Zhang, Z.H., Wei, D.E., Zhao, J.J., Kong, F., Cheng, G.H., et al., 2012. Implantation of mesenchymal stem cells improves right ventricular impairments caused by experimental pulmonary hypertension. Am. J. Med. Sci. 343, 402–406.
Martelli, A.M., Evangelisti, C., Chiarini, F., Grimaldi, C., Cappellini, A., Ognibene, A., et al., 2010. The emerging role of the phosphatidylinositol 3-kinase/Akt/mammalian target of rapamycin signaling network in normal myelopoiesis and leukemogenesis. Biochim. Biophys. Acta 1803, 991–1002.
Masri, F.A., Xu, W., Comhair, S.A., Asosingh, K., Koo, M., Vasanji, A., et al., 2007. Hyperproliferative apoptosis-resistant endothelial cells in idiopathic pulmonary arterial hypertension. Am. J. Physiol. Lung Cell Mol. Physiol. 293, L548–54.
Mattocks, A.R., Jukes, R., Brown, J., 1989. Simple procedures for preparing putative toxic metabolites of pyrrolizidine alkaloids. Toxicon 27, 561–567.
Moya, M.L., Cheng, M.H., Huang, J.J., Francis-Sedlak, M.E., Kao, S.W., Opara, E.C., et al., 2010. The effect of FGF-1 loaded alginate microbeads on neovascularization and adipogenesis in a vascular pedicle model of adipose tissue engineering. Biomaterials 31, 2816–2826.
Murphy, M., Drago, J., Bartlett, P.F., 1990. Fibroblast growth factor stimulates the proliferation and differentiation of neural precursor cells in vitro. J. Neurosci. Res. 25, 463–475.
Rabinovitch, M., 2012. Molecular pathogenesis of pulmonary arterial hypertension. J. Clin. Invest. 122, 4306–4313.
Shi, H., Cheng, Y., Ye, J., Cai, P., Zhang, J., Li, R., et al., 2015. bFGF Promotes the migration of human dermal fibroblasts under diabetic conditions through reactive oxygen species production via the PI3K/Akt-Rac1- JNK pathways. Int. J. Biol. Sci. 11, 845–859.
Shin, S., Kim, Y., Jeong, S., Hong, S., Kim, I., Lee, W., et al., 2013. The therapeutic effect of human adult stem cells derived from adipose tissue in endotoxemic rat model. Int. J. Med. Sci. 10, 8–18.
Thenappan, T., Ryan, J.J., Archer, S.L., 2012. Evolving epidemiology of pulmonary arterial hypertension. Am. J. Respir. Crit. Care Med. 186, 707–709.
Tsutsumi, S., Shimazu, A., Miyazaki, K., Pan, H., Koike, C., Yoshida, E., et al., 2001. Retention of multilineage differentiation potential of mesenchymal cells during proliferation in response to FGF. Biochem. Biophys. Res. Commun. 288, 413–419.
Tuder, R.M., Abman, S.H., Braun, T., Capron, F., Stevens, T., Thistlethwaite, P.A., et al., 2009. Development and pathology of pulmonary hypertension. J. Am. Coll. Cardiol. 54, S3–9.
Tuder, R.M., Chacon, M., Alger, L., Wang, J., Taraseviciene-Stewart, L., Kasahara, Y., et al., 2001. Expression of angiogenesis-related molecules in plexiform lesions in severe pulmonary hypertension: evidence for a process of disordered angiogenesis. J. Pathol. 195, 367–374.
Tuder, R.M., Groves, B., Badesch, D.B., Voelkel, N.F., 1994. Exuberant endothelial cell growth and elements of inflammation are present in plexiform lesions of pulmonary hypertension. Am. J. Pathol. 144, 275–285.
Virag, J.A., Rolle, M.L., Reece, J., Hardouin, S., Feigl, E.O., Murry, C.E., 2007. Fibroblast growth factor-2 regulates myocardial infarct repair: effects on cell proliferation, scar contraction, and ventricular function. Am. J. Pathol. 171, 1431–1440.
Wang, Z., Wang, Y., Ye, J., Lu, X., Cheng, Y., Xiang, L., et al., 2015. bFGF attenuates endoplasmic reticulum stress and mitochondrial injury on myocardial ischaemia/reperfusion via activation of PI3K/Akt/ERK1/2 pathway. J. Cell. Mol. Med. 19, 595–607.
Weichhart, T., Saemann, M.D., 2008. The PI3K/Akt/mTOR pathway in innate immune cells: emerging therapeutic applications. Ann. Rheum. Dis. 67 (Suppl 3), iii70–4.
Yanez, R., Lamana, M.L., Garcia-Castro, J., Colmenero, I., Ramirez, M., Bueren, J.A., 2006. Adipose tissue-derived mesenchymal stem cells have in vivo immunosuppressive properties applicable for the control of the graft-versus-host disease. Stem Cells 24, 2582–2591.
Zhang, H., Li, H., Yang, L., Deng, Z., Luo, H., Ye, D., et al., 2013. The ClC-3 chloride channel associated with microtubules is a target of paclitaxel in its induced-apoptosis. Sci. Rep. 3, 2615.
Zhao, T., Qi, Y., Li, Y., Xu, K., 2012. PI3 Kinase regulation of neural regeneration and muscle hypertrophy after spinal cord injury. Mol. Biol. Rep. 39, 3541–3547.
Zuk, P.A., Zhu, M., Mizuno, H., Huang, J., Futrell, J.W., Katz, A.J., et al., 2001. Multilineage cells from human adipose tissue: implications for cell-based therapies. Tissue Eng. 7, 211–228.